

Efficient Dibenzo[*c*]acridine Helicene-like Synthesis and Resolution: Scaleup, Structural Control, and High Chiroptical Properties

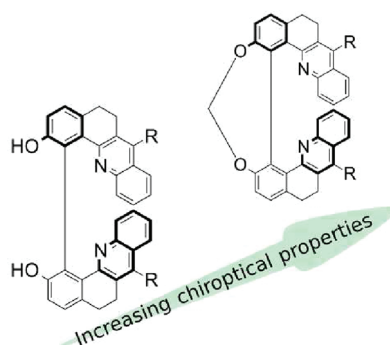
Loïc Jierry,[†] Steven Harthong,[‡] Christophe Aronica,[‡] Jean-Christophe Mulatier,[‡] Laure Guy,^{*,‡} and Stéphan Guy[§]

Institut Charles Sadron (UPR22-CNRS), 23 rue du Loess, BP 84047, 67034 Strasbourg Cedex 2, France, ICS (UPR22-CNRS), Laboratoire de Chimie Ecole Normale Supérieure de Lyon 46, Allée d'Italie, 69364 Lyon Cedex 07, France, and LPCML Université Lyon 1, UMR 5620, 69622 Villeurbanne, France

*laure.guy@ens-lyon.fr

Received November 14, 2011

ABSTRACT



Herein, we describe our recent expeditious synthesis of dibenzo[*c*]acridine helicene-like compounds on a large scale in pure enantiomeric form. This flexible synthesis allows for variation at several positions on the skeleton. Geometrical parameters related to these compounds have been obtained from monocrystal X-ray structure resolution. Additionally, chiroptical parameters have been recorded, highlighting the versatility of this family showing for example optical rotation at 589 nm varying between 135 and 150 deg g⁻¹cm².

Molecules from the helicene family (helicene-like) make up a unique class of compounds due to their uncommon capabilities in enantioselective catalysis,¹ molecular

recognition,² nonlinear optics,³ and their use as liquid crystals⁴ or components for molecular devices.⁵ Helicenes are also of prime importance for the quest to manufacture high optical rotation (OR) materials. Research for these materials is driven by the many potential applications predicted in different papers.⁶ For example, we have recently demonstrated that chirowaveguides— isotropic planar chiral waveguides⁷—are ideal for use as universal

[†] Institut Charles Sadron.

[‡] ENS Lyon.

[§] LPCML.

(1) (a) Dreher, S. D.; Katz, T. J.; Lam, K. C.; Rheingold, A. L. *J. Org. Chem.* **2000**, *65*, 815–822. (b) Nakano, D.; Hirano, R.; Yamaguchi, M.; Kabuto, C. *Tetrahedron Lett.* **2003**, *44*, 3683–3686.

(2) (a) Nuckolls, C.; Katz, T. J.; Katz, G.; Collings, P. J.; Castellanos, L. *J. Am. Chem. Soc.* **1999**, *121*, 79–88. (b) Honzawa, S.; Okubo, H.; Anzai, S.; Yamaguchi, M.; Tsumoto, K.; Kumagai, I. *Bioorg. Med. Chem.* **2002**, *10*, 3213–3218. (c) Amemiya, R.; Yamaguchi, M. *Org. Biomol. Chem.* **2008**, *6*, 26–35. (d) Senechal-David, K.; Toupet, L.; Maury, O.; Le Bozec, H. *Cryst. Growth Des.* **2006**, *6*, 1493–1496.

(3) Verbiest, T.; Van Elshocht, S.; Persoons, A.; Nuckolls, C.; Phillips, K. E.; Katz, T. J. *Langmuir* **2001**, *17*, 4685–4687.

(4) Nuckolls, C.; Shao, R. F.; Jang, W. G.; Clark, N. A.; Walba, D. M.; Katz, T. J. *Chem. Mater.* **2002**, *14*, 773–776.

(5) Kelly, T. R.; Sestelo, J. P.; Tellitu, I. *J. Org. Chem.* **1998**, *63*, 3655–3665.

(6) (a) Lindell, V. I.; Shivola, A.; Tretyakov, S.; Viitanen, A. *Electromagnetic waves in Chiral and Bi-Isotropic Media*; Artech House: 1994. (b) Mazur, J.; Mrozowski, M.; Okoniewski, M. *J. Opt. Soc. Am. B* **1992**, *9*, 641–650.

chiral sensors.⁸ However, all of these applications require as a first step the synthesis of a chiral material with high OR and transparency, a task difficult to fulfill due to the Kramers–Kronig (KK) transforms.⁹ In the case of chiral sensors, the spectral window of interest is the visible region because most targeted chiral analytes (natural compounds, drugs, etc.) only have significant optical activity in this part of the electromagnetic spectrum.

The [6]-helicene with $[\alpha]_D = 3640$ and an absorption tail-off wavelength in the UV at ~ 370 nm would be a good target if its synthesis were efficient. Additionally, the $[\alpha]_D$ of conjugated [*n*]-helicenes increases with the number of rings (*n*),¹⁰ but as a consequence of KK relations, the absorption wavelength is red-shifted, making them unsuitable for use in the manufacture of visible-region chirodevices. More generally for material design, and for whichever the spectral window targeted, helicenes have two unworkable drawbacks: the difficulties of their synthesis and their low racemization barrier.¹¹

Many original strategies for the synthesis of helical molecules are reported in the literature: photochemical,¹² Friedel and Craft,¹³ Diels–Alder,¹⁴ metal-catalyzed coupling, or cycloaddition,^{15,16} reactions. Unfortunately they have rarely been scaled up to gram production.¹⁷ To tackle this issue, we have designed a simple reaction pathway based on the use of easily accessible units featuring strong chromophores, and their coupling as a helicene-like structure via two key steps known for their efficiency: the aryl–aryl homocoupling and the bridging between phenolic functions. Finally, the resulting schematic framework (Figure 1) features four strong interacting chromophores, two phenyls (Ph) and two quinolyls (Qui). These chromophores display strong electronic transitions in the UV part and none in the visible part of the spectrum. Moreover, associating the chromophores closely in space via the helical skeleton induces strong resonant exciton coupling and thus gives rise to a striking chiroptical response. The inclusion of these moieties permits the modulation of the chiroptical properties by modification of the phenyl unit

functionalization and by the nature of the bridge. While few structure vs optical rotation studies are described in the literature,^{15,18} this work affords new elements in this direction.

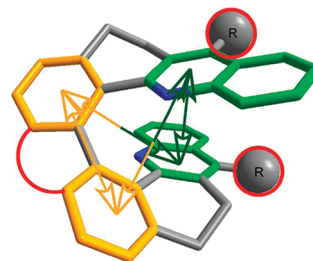


Figure 1. Schematic view of the molecules showing the main chiral interactions between chromophores (arrows) and the adjustable structural parameters (red) involved in the chiroptical properties.

The synthetic pathway (Scheme 1) starts with the Friedländer cyclization between 6-bromo-7-methoxy tetralone **1**¹⁹ and the hydrochloride of aminobenzophenone or aminoacetophenone. It gives the 1-bromo-2-methoxy-5,6-dihydrobenzo[*c*]acridine unit **2** substituted at position 7 with an excellent yield (90%) if R = Ph (**2b**) and a lower one (35%) when R = Me (**2a**), due to side reactions resulting from the presence of α -hydrogens belonging to the carbonyl in the latter case. The Ullmann's homocoupling of **2** provides the expected biaryl structure **3**. At this stage, we chose to continue with the most easily accessible Ph derivative (**3b** R = Ph (88%) vs **3a** R = Me (42%)). Demethoxylation of **3b** is quantitatively achieved upon treatment with tetramethylsilyl iodide and affords the protonated biphenol derivative **4b**. Finally, the standard procedure reported for binol chemistry afforded a methylene bridged compound **5b** with a 94% yield. As it relies on two very powerful and easy to handle reactions, the Friedländer reaction²⁰ for the monomer construction and the Ullmann coupling for the dimerization,²¹ the racemic synthesis of this dibenzo[*c*]acridine compound **5b** is easy and efficient (75% overall yield in four steps). Notably, it can yield up to 5 g of the R = Ph derivative.

Racemic **3**, **4**, and **5** all crystallize in centrosymmetric space groups, exhibiting no spontaneous resolution behavior unlike that which is frequently observed in helicene frameworks (see Table 1 and the Supporting Information (SI)). One highlights that the targeted compounds of this study have an important tendency to fold into an helical shape in the solid state even if the structure is not enforced

(7) Engheta, N.; Pelet, P. *Opt. Lett.* **1989**, *14* (11), 593–5.
 (8) Guy, S.; Bensal-Ledoux, A.; Stoita-Crisan, A. *PIER B* **2010**, *24*, 155–172.
 (9) Krykunov, M.; Kundrat, M. D.; Autschbach, J. *J. Chem. Phys.* **2006**, *125*, 194110.
 (10) Meurer, K.; Vogtle, F. *Organic Chemistry: Topics in Current Chemistry*; Springer: Berlin/Heidelberg, 1985; Vol. 127; pp 1–76, 10.1007/BFb0049438.
 (11) Rajca, A.; Rajca, S.; Pink, M.; Miyasaka, M. *Synlett* **2007**, 1799, 1822.
 (12) Jorgensen, K. B. *Molecules* **2010**, *15*, 4334–4358.
 (13) (a) Ichikawa, J.; Yokota, M.; Kudo, T.; Umezaki, S. *Angew. Chem., Int. Ed.* **2008**, *47*, 4870–4873. (b) Field, T. J.; Hill, J. E.; Venkataraman, D. *J. Org. Chem.* **2003**, *68*, 6071–6078.
 (14) (a) Wang, D. Z.; Katz, T. J. *J. Org. Chem.* **2005**, *70*, 8497–8502. (b) Carreño, M. C.; González-López, M.; Urbano, A. *Chem. Commun.* **2005**, 611–613.
 (15) Nakano, K.; Hidehira, Y.; Takahashi, K.; Hiyama, T.; Nozaki, K. *Angew. Chem., Int. Ed.* **2005**, *44*, 7136.
 (16) (a) Mamane, V.; Hannen, P.; Furstner, A. *Chem.–Eur. J.* **2004**, *10*, 4556–4575. (b) Sehnal, P.; Stará, I. G.; Saman, D.; Tichý, M.; Mišek, J.; Cvačka, J.; Rulišek, L.; Chocholoušová, J.; Vacek, J.; Goryl, G.; Szymonski, M.; Cisařová, I.; Starý, I. *Proc. Natl. Acad. Sci. U.S.A.* **2009**, *106*, 13169–13174.
 (17) Paruch, K.; Vyklický, L.; Katz, T. J.; Incarvito, C. D.; Rheingold, A. L. *J. Org. Chem.* **2000**, *65*, 8774–8782.

(18) (a) Grimme, S.; Harren, J.; Sobanski, A.; Vogtle, F. *Eur. J. Org. Chem.* **1998**, 1491, 1509. (b) Rajca, A.; Pink, M.; Xiao, S.; Miyasaka, M.; Rajca, S.; Das, K.; Plessel, K. *J. Org. Chem.* **2009**, *74*, 7504–513.
 (19) Bohlmann, F.; Fritz, G. *Chemische Berichte-recueil* **1976**, *109*, 3371–3374.
 (20) Marco-Contelles, J.; Perez-Mayoral, E.; Samadi, A.; Carreiras, M. D.; Soriano, E. *Chem. Rev.* **2009**, *109*, 2652–2671.
 (21) Hassan, J.; Seignion, M.; Gozzi, C.; Schulz, E.; Lemaire, M. *Chem. Rev.* **2002**, *102*, 1359–1469.

Table 1. X-ray Crystal Structures of (\pm)-**3a**, (\pm)-**3b**, (\pm)-**4b**, and (\pm)-**5b** Which Show Face and Side Elevations (H-atoms are omitted for clarity; red, O; blue, N)^a

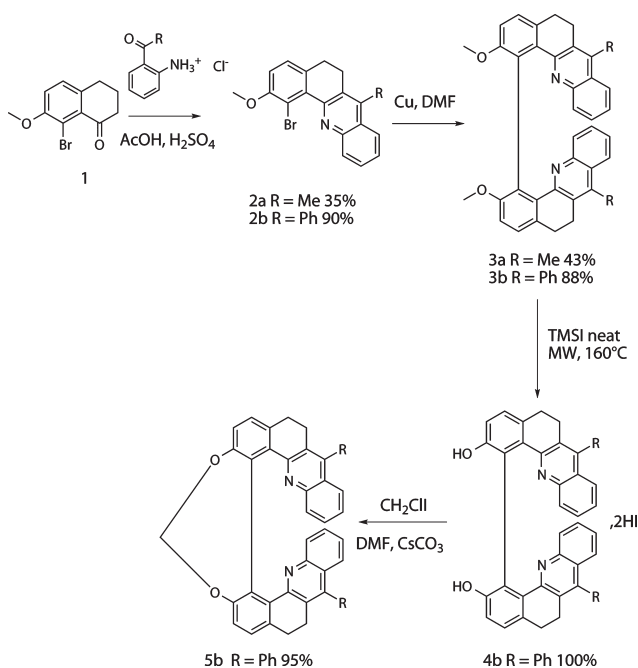
	3a	3b	4b	5b
X-Ray structures				
Space group θ	Triclinic, <i>P1</i> 64°	Triclinic, <i>P2₁/a</i> 89°	Monoclinic, <i>C2/c</i> 67°	Orthorhombic, <i>Pcan</i> 47°

^a θ : Biphenyl torsion angles.

by a bridge (**3** and **4**). The variation in conformations is mainly governed by the change in the biphenyl torsional angle θ which varies from 47° to 89° through the series (clearly visible in the side view in **1**). On the other hand, the conformation of the benzo[*c*]acridine subunit remains almost the same with the value of the angle between the plane of the Ph and the Qui varying from 26° to 37°.

The enantiomeric resolution of **4b** is carried out by the separation of the corresponding bis-menthyl carbonate diastereomers by column chromatography (Scheme 2). Each column delivers three fractions yielding 30% of the first eluted diastereomer (–)-**6b**, 30% of the second eluted diastereomer (+)-**6b** in pure form, and 30% of an intermediate mixed fraction that undergoes further chromatography. After the easy removal of the resolution auxiliary

Scheme 1. Racemic Synthetic Pathway of Dibenzo[*c*]acridine Helicene-like Compound **5b**



Scheme 2. Synthetic Pathway (–)-*M*-**5b** via Optical Resolution of *rac*-**4b**

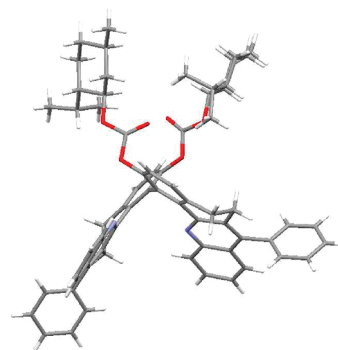
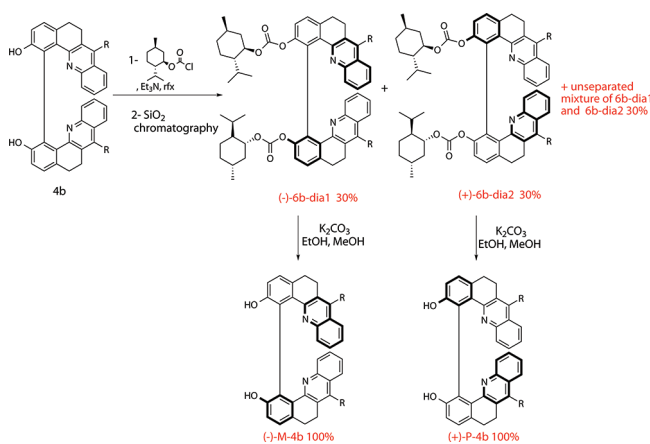


Figure 2. X-ray structure of (+)-**6b**.

using classical basic conditions ($K_2CO_3/MeOH$), pure enantiomers (+)-**4b** and (–)-**4b** are isolated on the 1 g scale. No loss of enantiomeric excess has been measured

during this step according to chiral HPLC analysis. Compounds **3a** and **3b** have been easily resolved by semipreparative HPLC (method described in the SI).

The X-ray structure resolution of a monocrystal of (+)-**6b** (Figure 2) allows us to assign the absolute configuration of the key intermediate **4b**.

The absolute configurations of all the compounds have been assigned both from the reliable absolute configuration of (–)-*M*-**4b** and by their individual CD spectra (Figure 3). Indeed, levorotatory enantiomers always exhibit positive bands centered around 205 and 265 nm and negative bands around 225, 240, and 288 nm that can be taken as a marker for a (–)-*M* (respectively (+)-*P*) configuration.

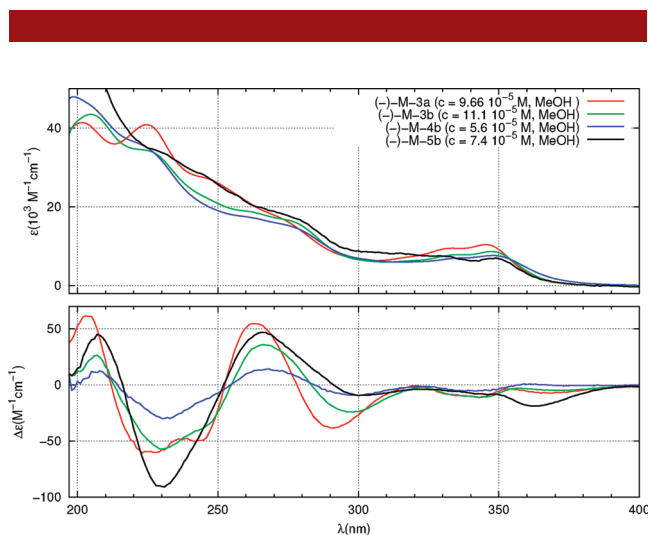


Figure 3. UV (upper panel) and CD (lower panel) spectra for **3a–b**, **4b**, and **5b** collected from methanol solutions.

Specific OR values $[\alpha]_D$ (10^{-1} deg $g^{-1}cm^2$) and molar OR values $[\Phi]_D$ (10^{-3} deg $mol^{-1}cm^2$) that better quantify the activity at a molecular level (Table 2) are higher than common chiral organic compounds except for the phenolic compound (+)-**4b** and are on the same order of magnitude as the value of *P*-[6]-carbohelicene ($[\Phi]_D = 11\,950$). The evolution of the OR vs the solid state geometrical parameters is not obvious and does not follow, for example, θ values. However, the evolution for the two similar derivatives *R* = Ph compounds **3b** and **5b** highlights the effect of the bridge (i.e., the geometrical constraint) on the chiroptical activity. Moreover, this bridge makes **5b** very much more stable toward thermal racemization than **3b**. Time-

(22) Martin, R. H.; Marchant, M. J. *Tetrahedron* **1974**, *30*, 347–349.

dependent racemization was monitored by HPLC analysis in diphenyl ether at 200 °C. While **3b** proceeds with values $t_{1/2} = 23.1$ h and $\Delta G = 39.7$ kcal/mol, comparable to [6]-helicene,²² **5b** presents no racemization after 93 h under the same conditions.

UV absorption and CD spectra (Figure 3) feature the typical bands of the Ph and Qui chromophores, 1L_b in the

Table 2. Specific OR ($[\alpha]_D$) and Molecular OR ($[\Phi]_D$) Measured in CH_2Cl_2 Solutions

	(+)- 3a	(+)- 3b	(+)- 4b	(+)- 5b
$[\alpha]_D$	+400	+703	+135	+1489
$[\Phi]_D$	+2201	+4731	+870	+9783

range 300–360 nm, 1L_a at 250 nm, and 1B_b around 210 nm.²³ CD spectra are dominated by two opposite bisignate couplets, a negative one centered at 210 nm and a positive one at 250 nm for the *M* configuration. It should be noted that the intensity of the CD_{230nm} signal roughly follows the optical activity measured at 589 nm. The 230 nm region exhibits an overlapping of bands depending on the molecular structure. **3a** presents a significant resolution of the two opposite CD couplets at 210 and 250 nm. The resolution of these two couplets is lower for **3b** and is lost for **4b** and **5b**. Finally, the higher the overlap, the bigger the OR.

In summary, we have described the first effective scaled-up development syntheses of helicene-like molecules having a dibenzo[*c*]acridine skeleton in an optically pure form with high OR and have assigned their helicities. The molecular structure can be easily tuned by changing the substitutions, thus featuring very different chiroptical properties (OR at 589 nm tuned between 135 and 1500).

Moreover, these molecules are configurationally stable at room temperature and transparent in the visible part of the spectrum, making them very promising candidates for further application in chiroptical science.

Acknowledgment. We thank the ANR (Project GUI-CHIELI 08-BLAN-0149) for its financial support.

Supporting Information Available. Experimental procedures and characterization data for all new compounds. This material is available free of charge via the Internet at <http://pubs.acs.org>.

(23) (a) Blakemore, P. R.; Kilner, C.; Milicevic, S. D. *J. Org. Chem.* **2006**, *71*, 8212–8218. (b) Sagiv, J.; Yogev, A.; Mazur, Y. *J. Am. Chem. Soc.* **1977**, *99*, 6861–6869.